SPIXIANA	48	1	15-30	München, November 2025	ISSN 0341-8391
----------	----	---	-------	------------------------	----------------

# Structural insights into branchiopod cysts comparing µCT, SEM, and light microscopy

(Crustacea: Branchiopoda: Anostraca, Notostraca, Diplostraca)

# Christian Vogelmann, Hans Pellmann, Noha Wlocka & Martin Heß

Vogelmann, C., Pellmann, H., Wlocka, N. & Heß, M. 2025. Structural insights into branchiopod cysts comparing  $\mu$ CT, SEM, and light microscopy (Crustacea: Branchiopoda: Anostraca, Notostraca, Diplostraca). Spixiana 48(1): 15–30.

The cysts (resting embryos) of ten branchiopod species have been investigated with light and scanning electron microscopy and tomographic x-ray microscopy, as well. In a comparative manner we show characters like colour, shape, diameter, surface texture, internal layering of the cells, as well as shape and surface structure of the embryo. The advantages and disadvantages of the three methods are discussed, as well as the significance of the investigated structures in terms of taxonomy, evolutionary and ecological aspects, and shrinkage effects upon drying.

Christian Vogelmann (corresponding author), Bayerische Landesanstalt für Landwirtschaft, Institut für Fischerei, Weilheimer Str. 8, 82319 Starnberg, Germany; e-mail: christian.vogelmann@lfl.bayern.de

Hans Pellmann & Noha Wlocka, Museum für Naturkunde, Otto-von-Guericke-Str. 68–73, 39104 Magdeburg, Germany

Christian Vogelmann & Martin Heß, Biozentrum LMU München, Zoologie, Großhaderner Str. 2, 82152 Planegg-Martinsried, Germany

Martin Heß (corresponding author), GeoBio Center LMU München, Richard-Wagner-Str. 10, 80333 München, Germany; e-mail: hess@bio.lmu.de

#### Introduction

Large branchiopods, a group of freshwater crustaceans, are notable for their ability to produce cysts, also known as "resting eggs", which enable them to withstand challenging environmental conditions. These cysts are integral to their life cycle, particularly for species living in ephemeral freshwater habitats like seasonal ponds, rain pools, and floodplains that were dry for the most time for one or several years (Engelmann & Hahn 2004). They serve as a crucial mechanism for populations to endure environmental fluctuations, including desiccation and extreme salinity (Wang & Chou 2015, Mabidi et al. 2017). Additionally, adaptations such as short generation cycles facilitate rapid population growth during favourable conditions (Gottwald & Hödl 1996, Burmeister 2000).

Their global distribution ranges from desert regions to Mediterranean wetlands and even Arctic tundra. In Europe, particularly in Mediterranean and temperate zones, they are commonly found in ephemeral wetlands and floodplains that fill with water during spring or after heavy rains. In Germany, all species of large branchiopods are listed as endangered on the Red List (Simon 2016), with habitat loss due to human activities posing a significant threat (Rieder et al. 1979). However, they are increasingly observed in secondary habitats like carp ponds and tire tracks on military training grounds, demonstrating their adaptability to changing environments (Wüstemann & Nicolai 2012, Vogelmann et al. 2021a).

The cysts encase embryos in a state of developmental arrest at the gastrula stage, maintaining a minimal metabolic activity that enables the embryos to survive unfavorable conditions, including extreme temperature, desiccation, and salinity, over extended periods (Wiggins et al. 1980, Clegg 1997, Glandt 2006). When favourable conditions arise – typically when these ephemeral habitats refill with water – embryonic development resumes, and within hours, the embryo transforms into a nauplius larva, hatching from the protective shell and beginning its active life cycle.

Cysts display notable variation in size and morphology across species, though the biological significance of these differences is not yet well understood. Once laid and dried, resting eggs exhibit species-specific shapes, structures, and sizes, which can often aid in identifying the species (Mura 1986, Thiéry et al. 1995).

This study aims to compare the effectiveness of three imaging techniques – binocular light microscopy, scanning electron microscopy (SEM), and micro-computed tomography (µCT) – to analyse the cyst morphology of nine species of large branchiopods found in Germany, including five Anostraca, two Notostraca, and three Diplostraca/Spinicaudata species. Among these, *Chirocephalus carnuntanus*, an Anostraca species, represents a new discovery in Germany (publication Driechciaz et al. 2025), while *Artemia monica* (formerly known as *A. franciscana*) was included as a reference for comparative

purposes. The goal is to assess the advantages and limitations of each imaging technique, determining their utility for taxonomic and ecological research on large branchiopods. A further objective was to present these findings in a museum exhibition to make the scientific results accessible to a broader audience, with a focus on explaining the structure, function, and ecological significance of the cyst stage in the branchiopod life cycle.

#### Material and methods

Living animals were kept in aquaria under room temperatures, separated by species. The initial specimens included both, recent wild-caught individuals and breeding from these specimens (Table 1) except Artemia monica (breeding line nyos). The cysts deposited by females are denser than water, causing them to sink to the bottom, where they can be collected. To remove most foreign particles, the cyst-water mixture was repeatedly rinsed with tap water. After rinsing, the cyst-water suspension was drawn up with a pipette and transferred dropwise onto cellulose paper. While still damp, the cysts were separated from any remaining foreign matter using a fine paint brush or dissecting needle. The cysts placed on cellulose paper were then dried at room temperature and transferred into labeled collection vials. This preparation allows easy retrieval of cysts for future studies: once the cellulose is moistened, the cysts can be

**Table 1.** Collection data of the investigated species and their systematic position according to Olesen (2007) and Olesen & Richter (2013).

	Place of origin	Collection date
Anostraca		
Artemia monica (Verrill, 1869)	commercial Kosmos breeding set	(2024)
Branchipus schaefferi (Fischer, 1834)	Saxony-Anhalt, Colbitz-Letzlinger Heide military training area	June/July 2021
Eubranchipus grubii (Dybowski, 1860)	Saxony-Anhalt, Elbe flood pond near Magdeburg-Randau	April 2021
Chirocephalus carnuntanus (Brauer, 1877)		March 2024
Tanymastix stagnalis (Linnaeus, 1758)	Baden-Württemberg, Lake Eichen	April 2018, breeding: 2021
Phyllopoda		
Notostraca		
Triops cancriformis (Bosc, 1801)	Saxony-Anhalt, Colbitz-Letzlinger Heide military training area	2021
Lepidurus apus (Linnaeus, 1758)	Lower Saxony, near Eilte/Bierd	May 2023
Diplostraca		
Leptesteria dahalacensis (Rüppell, 1837)	Mixed sample: Austria, Blumengangsenke and Germany, Hesse, Fischzucht Stähler/Hadamar	2011 and 2015, breeding: July 2022
Cyzicus sp. (genus in revision)	Bavaria (Upper Palatinate), 2022	breeding: March 2023
Limnadia lenticularis (Linnaeus, 1761)	Mixed sample: Saxony, Königswartha and Baden-Württemberg, Au am Rhein	breeding: October 2022

easily lifted using a fine needle or brush and transferred to an appropriate specimen holder. This procedure was used for all species except *Lepidurus apus*. Freshly laid cysts of *L. apus* are sticky, often becoming coated with substrate particles, which adhere firmly to the cyst's surface, sometimes completely covering it. Attempts to remove these particles risk damaging the cyst shell or its adhesive layer. Therefore, an alternative approach was tested in which animals were kept without substrate; however, this resulted in a low cyst yield, likely because the floating adult animals consumed the cysts.

All analyses were conducted on air-dried cysts kept under room conditions. For the analyses, intact native cysts were used. Additionally, some cysts were punctured with a fine needle to reveal the internal structure under the SEM.

# **Imaging**

1. Light microscopy. Images were taken on an Olympus SZX 7 stereomicroscope with an DF PLAPO 1 x-4 lens at zoom position 5.6 x, illuminated with a Schott KL 1500 cold light source (ring light) at a colour temperature of 3400 K and an additional lateral gooseneck light (KL 1500). With an Olympus DP25 digital colour camera and the cell D 2.6 software (Olympus Soft Imaging Solutions) images with pixel dimensions of 1700 x 1200 px were grabbed (RGB images in JPG format without compression, white balanced on white paper). A calibrated stage micrometer slide was used to determine the correct pixel size.

**2. SEM.** For SEM, cysts were dropped on appropriate aluminium stubs with carbon adhesive tabs and covered with a 6 nm gold layer using a Leica EM ACE200 sputter coater. The samples were investigated on an Apreo VS field emission scanning electron microscope (ThermoFisher) at 5 kV, 0.1 nA beam current, 1–3 µs pixel dwell time, Everhart-Thornley-Detector for secondary electrons. Depending on the motive the pixel size ranged between 1.35 nm and 135 nm, pixel dimensions 6144×4376 px, 16-bit greyscale (not all images shown).

**3.** μCT. The dry cysts of the large branchiopod species (except *C. cranuntanus* and *A. monica*) were fixed on toothpicks (left on the cellulose paper or glued at one edge in case of *T. stagnalis*) and tomographic scans were performed with a Zeiss Xradia 410 Versa 3D x-ray microscope (Universität Rostock, Institut für Biowissenschaften, Allgemeine und Spezielle Zoologie, AG Prof. Dr. S. Richter) with the generation parameters shown in Table 2.

For *L. apus* the 20x objective was used, for all other species the 40x objective, 1 image per projection angle, camera binning 2. After backprojection of the raw data, eight image stacks of the following dimensions were exported (16-bit greyscale) (Table 3).

#### Digital image processing

The μCT image stacks were processed using Amira 5.6 software. After data import and adjusting the correct voxe size, the structures of interest, i.e. (1) cysts-shell and (2) developing embryo, were segmented for surface

Species	kV	W	Sector [°]	Voxel size [µm]	Exposure time [s]	Number of projections
Branchipus schaefferi	40	8	182	0.57	6	921
Eubranchipus grubii	40	8	182	0.57	6	921
Tanymastix stagnalis	40	8	182	0.58	12	1101
Triops cancriformis	50	8	182	0.58	12	941
Lepidurus apus	30	5	184	1.11	5	901
Leptestheria dahalacensis	40	8	182	0.57	6	921
Cyzicus sp.	50	8	182	0.57	6	861
Limnadia lenticularis	40	8	182	0.57	6	921

**Table 3.** X-ray microscopic stacks.

Species	Pixel dimensions	Object on N planes	Voxel size [μm]
Branchipus schaefferi	473 x 485 x 950	410	0.57 isotropic
Eubranchipus grubii	621 x 629 x 952	571	0.57 isotropic
Tanymastix stagnalis	$850 \times 1950 \times 1903$	1702	0.58 isotropic, 0.215 for reconstr.
Triops cancriformis	705×975×670	597	0.67 isotropic
Lepidurus apus	534 x 485 x 490	360	1.1 x 1.1 x 1.375
Leptestheria dahalacensis	$360 \times 321 \times 953$	151	0.57 isotropic
Cyzicus sp.	275 x 358 x 315	275	0.57 isotropic
Limnadia lenticularis	403 x 397 x 948	307	0.57 isotropic

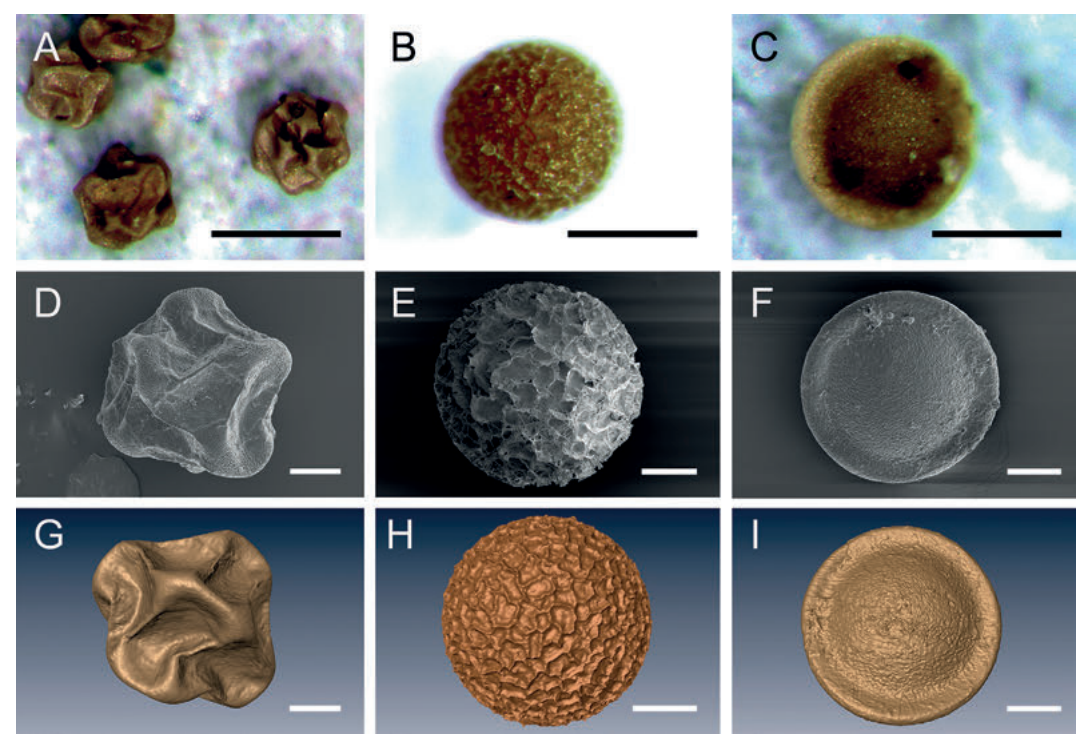


Fig. 1. External outer morphology of branchiopod cysts: Anostraca. A, D, G. Branchipus schaefferi; B, E, H. Eubranchipus grubii; C, F, I. Tanymastix stagnalis; A, B, C. light microscopy; D, E, F. scanning electron microscopy; G, H, I. surface rendering based on micro computed tomography. Scale bars: A, B, C 250 μm; D, G 50 μm; E, F, H, I 100 μm.

rendering. This was effected partly by applying threshold-based segmentation (after introducing separators where the structures contacted the substratum), partly following their contours manually. Surface rendering was executed with slight smoothing to reduce surface roughness caused by the shape of digital voxels near the resolution limit. Snapshots of appropriate motives were exported as JPGs (partly applying the surface-cut tool) and volumetry was performed with the Amira material statistics tool based on the calibrated voxels.

SEM images have been optimized for brightness and contrast using Adobe PS CS6.

All images for the figures were converted to 8-bit greyscale or 24-bit RGB and adjusted to the appropriate size at 400 dpi to match the printing area.

# Results

The morphological characters of the cysts of the ten investigated species were visualized with lightmicroscopy, scanning electron microscopy, and  $\mu$ CT\* (\*except *Chirocephalus* and *Artemia*). The dry cysts, depending on the species, measured between approx. 100  $\mu$ m and 500  $\mu$ m in diameter and differed

in colour, size, shape, surface texture and also in their internal shell structure. For the description of the outer and inner cyst structures of the species studied, the findings from the three methods used were combined. Here are the results for all species studied:

### Branchipus schaefferi

The cysts have a bronze-brown hue and the shape of contracted polyeders with rounded corners and edges (somehow like crumpled paper balls; Fig. 1A). The measured diameters of the available material are between 170 and 210  $\mu m$  (depending on the angle of the measuring ruler with respect to the irregularly shaped cyst). Upon closer inspection (SEM) the entire cortex surface shows a dense regular pattern of small depressions (partly with plane bottom, partly pore-like openings; Figs 1D,2G) – nearestneighbour distances ca. 1–2  $\mu m$ . The cyst has a thick external shell, which has a layered structure. The internal shell structure (Fig. 2J,J') reveals a dense multilayered cortex layer of ca. 0.95  $\mu m$ , followed by a spongy network of fibres and cavities (alveolar

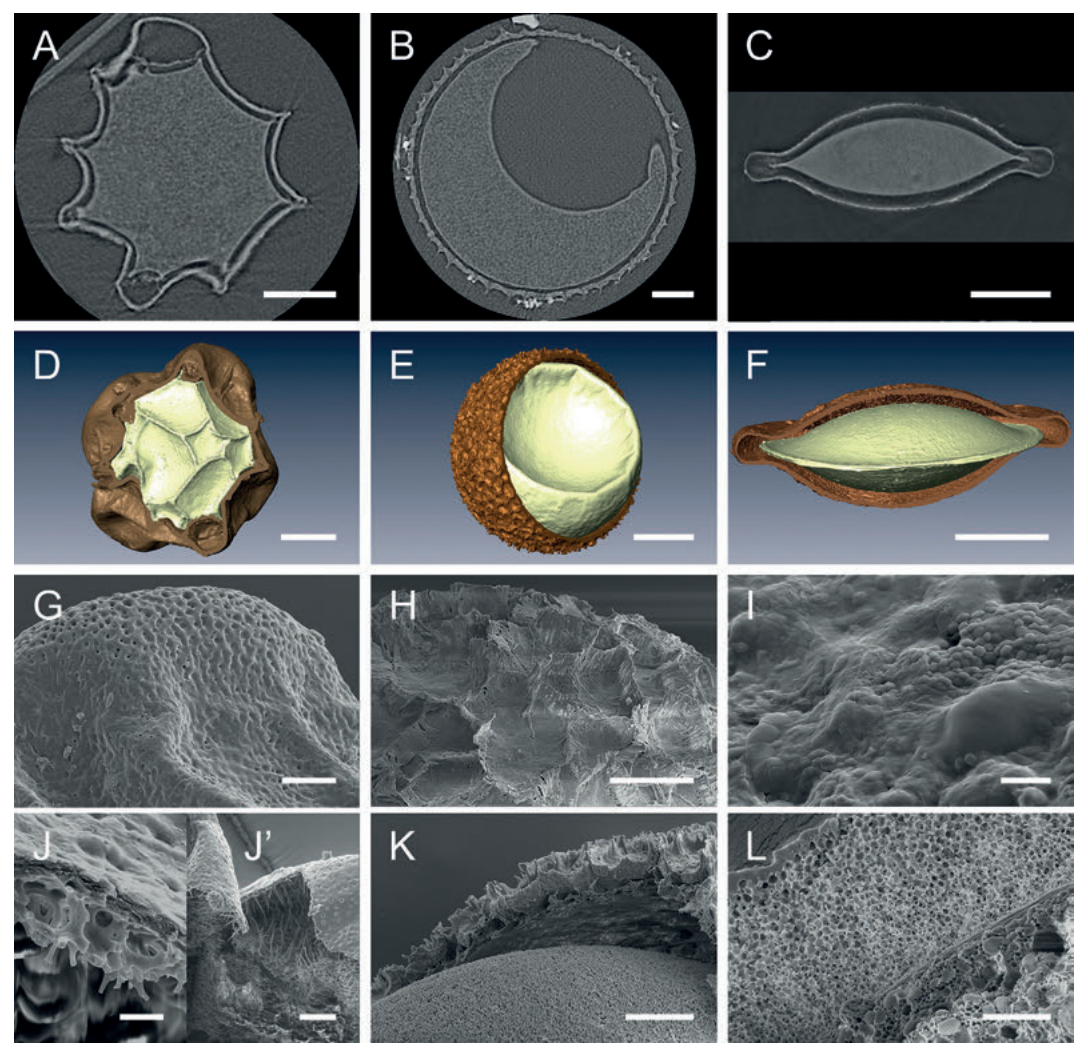


Fig. 2. Surface fine structure and inner structures of branchiopod cysts: Anostraca. A,D,G,J/J'. Branchipus schaefferi; B,E,H,K. Eubranchipus grubii; C,F,I,L. Tanymastix stagnalis; A,B,C. μCT selected plane; D,E,F. surface rendering based on μCT, cyst shell opened; G,H,I. cyst surface SEM; J/J',K,L. cyst shell fractured SEM. Scale bars: A,B,D,H 50 μm; C,E,F 100 μm; G,J',L 10 μm; I,J 2 μm; K 25 μm.

layer, ca.  $2.6 \, \mu m$  thick). A thin inner layer is indicated in Fig. 2J'. Below the rounded corners subcortical spaces with "detached" alveolar layer are found in which numerous elongated, pointed projections are extending from both sides (Fig. 2J'). Inside, the embryo appears as an unstructured mass that essentially follows the shape of the outer shell (Fig. 2A, D). The embryo surface (thin bright line in  $\mu$ CT according to an embryonic cuticle) adheres to the inner surface of the shell, with an "empty" space of about  $10 \, \mu m$ , except below the higher arches mentioned earlier, resulting in an irregular polyhedral shape with

concave planes and sharp ridges (Fig. 2D). In the broken SEM samples the embryo material shows lenticular structures of ca. 4  $\mu$ m diameter, at least at the surface (not shown). The embryo matrix appears irregularly granular, but superimposed by a less intense granular background artifact (Fig. 2A).

# Eubranchipus grubii

The cysts are globular with diameters between 340  $-375\,\mu m$  and a medium-brown colour (showing some glitter effects under the stereomicroscope,

Fig. 1B). The surface texture of the cyst shell is formed by a network of fine to very fine fibers that form densely arranged small basins with very thin walls (Figs 1E, 2H, K), vaguely reminiscent of the surface structure of hard corals like *Paramontastrea peresi*. In LM (Fig. 1B) and  $\mu$ CT (Fig. 1H) the walls appear less thin and more rounded. From Figure 2B ( $\mu$ CT) and 2K (SEM) it can possibly be concluded that the basins are largely independent cortical units sitting on top of alveolar chambers with clefts or pores in between. The inner boundary of the protective cyst shell is formed by a thin smooth layer of interwoven fibres (Fig. 2K).

The overall shape of the embryo inside is globular but finally cup-shaped due to a noticeable indentation (Fig. 2B, E). With a measured radius of 172 µm the volume of a globular embryo would be 0.023 mm<sup>3</sup>, the Amira volumetry delivers a result of 0.014 mm<sup>3</sup> for the segmented embryo material, tantamount to a volume loss of 1/3. The egg surface follows the inner shell surface with a small gap (max. 20 μm). The embryonic cuticle (indicated as thin bright line in µCT, Fig. 2B) has a thickness of ca. 2.5 µm (derived from SEM, not shown), with an outer surface fine structure reminiscent of minute tipped nipples (ca. 2  $\mu$ m long, 160/100  $\mu$ m<sup>2</sup>, Fig. 2K), like on the cornea surface of night-insect ommatidia but less regular. The embryo matrix is again granular, despite the superimposed granular background artifact (Fig. 2B).

# Tanymastix stagnalis

The cysts of *T. stagnalis* have a lentiform shape with a flattened outer margin (Figs 1C, F, I; 2C, F), diameter 365–380 μm, central height 120 μm. The colour is dark brown with a beige margin (Fig. 1C). The overall surface texture is smooth with irregularities in the range of 2 µm and smaller (Figs 1F, 2I). The three-layered structure of the cyst shell can be clearly seen in the SEM image (Fig. 2L): A thin compact surface layer made of oval structures (long axis up to 5 µm) in a homogenous matrix, is followed by a ca. 20 µm spongy ("alveolar") layer with small globular and interconnected cavities, demarcated by thin compact inner layer. The lentiform embryo shape follows the inner margin of the shell in a distance of ca. 40 µm (suspended by loose fibrous material as seen in µCT data) with a thin marginal ring (Fig. 2C, F). With 0.0027 mm<sup>3</sup> it fills 42.2 % of the entire cyst inner volume (0.0067 mm³). In μCT the embryo volume appears granular (3.5 µm structures in a less attenuating fine-granular matrix, Fig. 2C, F).

# Chirocephalus carnuntanus

The cysts are globular (diameter 220–240  $\mu m$ ), orange-yellow with greenish spots in places, and with a bristly rough surface (Fig. 3A). In the SEM the bizarrely shaped bristles (and some debris and diatom shells between their bases) can be seen clearly. Considering the very fine tips can result in a slightly larger total diameter (up to 260  $\mu m$ ) compared with LM. In the fractured preparation (Fig. 3E) one can see alveolar chambers below the spiny cortex separated by radial slits (cf. E. schaefferi), confined by a thin internal layer. The embryo inside appears only slightly cup-shaped with short hairs like structures on the surface (Fig. 3E). For this species no  $\mu CT$  scan is available.

#### Artemia monica

The cysts of are dark brown in colour (Fig. 3B). The shape is of a floppy ball of 190–210  $\mu m$  diameter, deeply dented on one side (Fig. 3B, D). The surface appears comparatively very smooth (also at high SEM magnifications) with the suggestion of an irregular honeycomb structure overlayed by a kind of hardly recognizable 1.5  $\mu m$  pavement. The inner fine structure of the shell consists of a thin compact cortex layer followed by a alveolar layer made of spongy material enclosing small spherical cavities (diameter 0.7–0.85  $\mu m$ , Fig. 3F), which are connected to the neighbours via small holes. The inner surface of the third, inner layer displays flat scales perforated by tiny holes (Fig. 3F). For this species no  $\mu CT$  scan is available.

# Triops cancriformis

The cysts are spherical (diameter 300-340 µm) with irregularly shaped shallow depressions (Fig. 4C, E). The diameter measured in different directions can vary 2-3%, the colour is a reddish dark-brown (Fig. 4A). The surface fine structure shows very small porous holes in the range between 50 and 200 nm (Fig. 5E). The layered structure of the cyst shell is clearly visible. It consists of a robust 2 µm cortex layer (radial pores visible in cracked samples) and an 28 µm alveolar layer composed of 7-10 µm bubbles (Fig. 5A, G), surrounded by continuous walls with very small holes connecting neighbouring units (zoom into Fig. 5G). The contact zone with the embryonal surface can be defined as inner layer. The embryo is spherical with a shrinkage dent, filling ca. 66 % of the cyst volume (derived from Amira volumetry). The embryonic cuticle is dense 2.4 µm thick layer, partly covered by material from the inner cyst layer with the corresponding pattern (Fig. 5G). The embryo volume contains many 2 µm granules in a spongy matrix (not shown, but see µCT aspect in Fig. 5A).

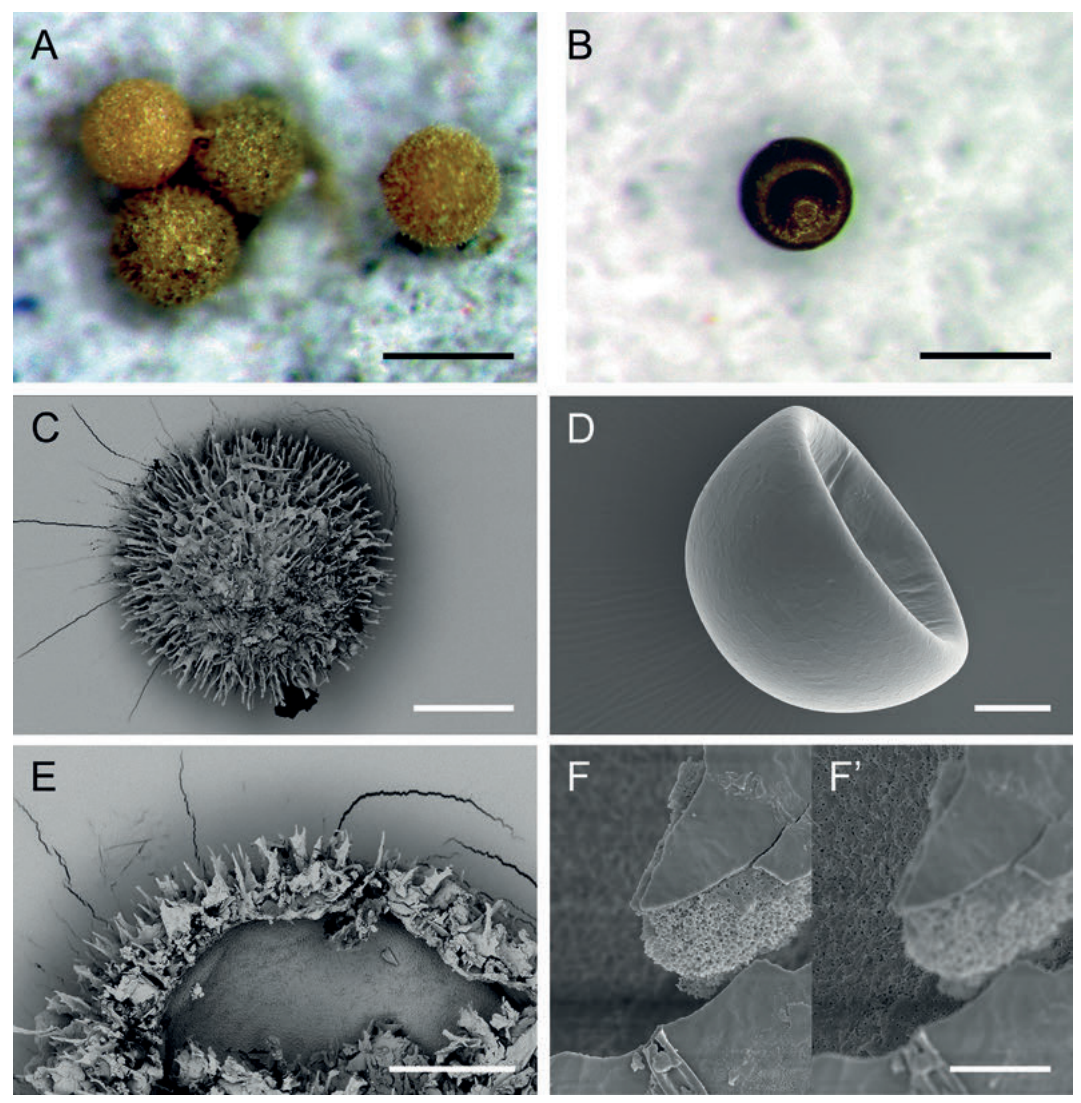


Fig. 3. Outer morphology of branchiopod cysts: Anostraca. A, C, E. Chirocephalus carnuntanus; B, D, F/F'. Artemia monica; A, B. light microscopy; C, D. scanning electron microscopy; E, F. surface rendering based on micro computed tomography. Scale bars: A, B 250 μm; C 100 μm; D, E 50 μm F/F' (two focus planes) 10 μm.

# Lepidurus apus

The basic colour of the cysts is a shiny dirty yellow, in the examined samples with green spots and small red dots (Fig. 4B). The overall shape is spherical, with more (Fig. 4F) or less (e.g. Fig. 4D) adherent material of unknown nature. The diameters are 475–500 µm – in the SEM sample diameter measurements in different directions exhibit variations of less than 0.2 %. The surface texture of the cortex layer is smooth with tiny holes in groups (Fig. 4D). The three layers of the

cysts shell have a thickness of 1  $\mu m$  (cortex), 9  $\mu m$  (alveolar) layer, and 9  $\mu m$  (inner layer, made of condensed granular material, see Fig. 5H). The surface of the embryonic cuticle appears rough, the inner matrix has the same appearance in  $\mu CT$  than e.g. in Triops.

#### Leptesteria dahalacensis

The dried cysts are semi-transparent, have a lemon yellow colour, and the shape of spheres (diameter 110–115 µm) with a large single shrinkage dent or

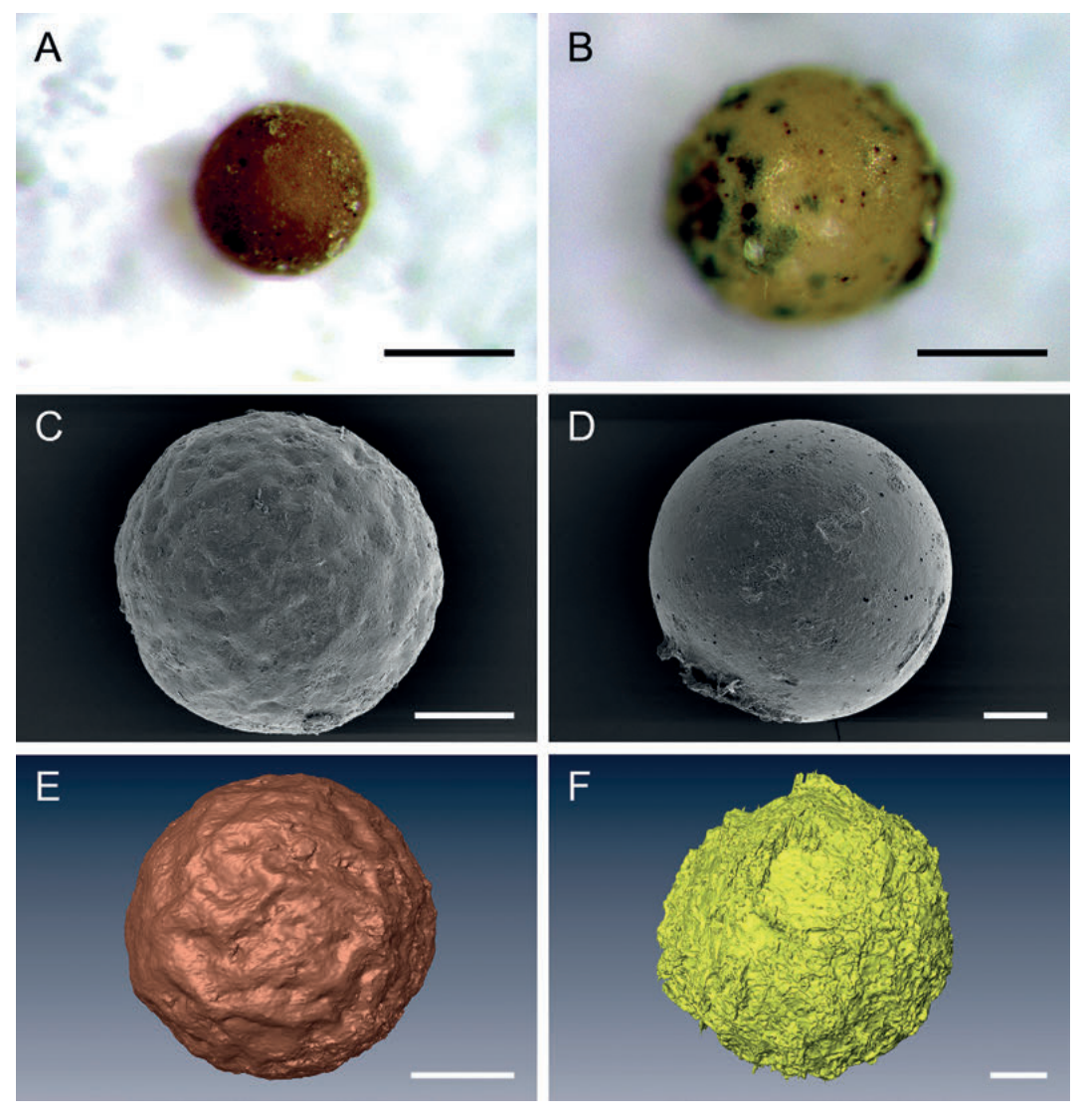
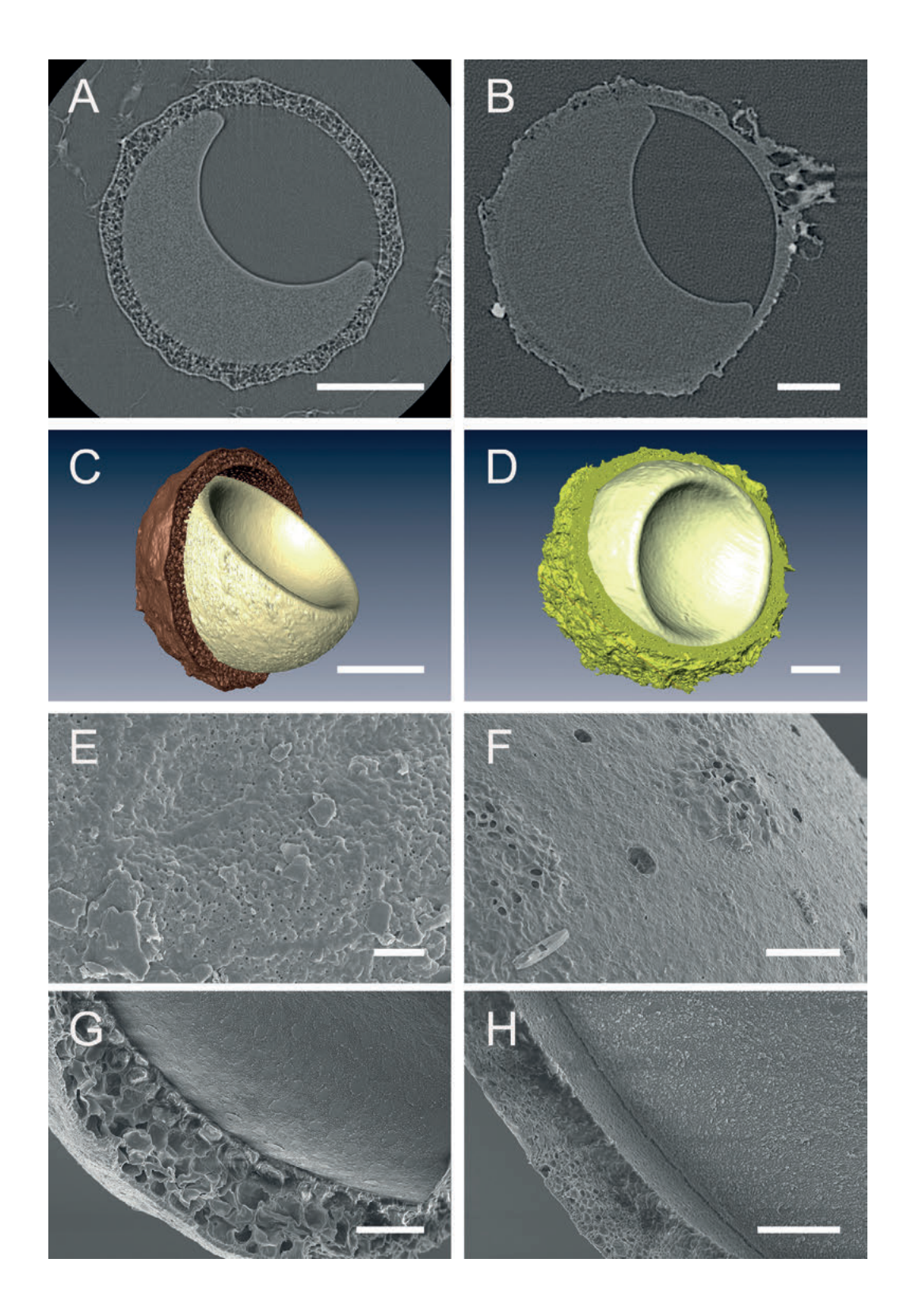


Fig. 4. Outer morphology of branchiopod cysts: Notostraca. A, C, E. *Triops cancriformis*; B, D, F. *Lepidurus apus*; A, B. light microscopy; C, D. scanning electron microscopy; E, F. surface rendering based on micro computed tomography. Scale bars: A, B 250 μm; C-F 100 μm.

other way round the shape of a hemisphere with a cup like triangular depression (Figs 6A,G; 7J). This can lead to a widening in one axis up to 120 µm (Fig. 6D,G). The surface of the cyst is exceptionally smooth (Fig. 7G). In a fractured SEM preparation

one can see shell of only 2–2.5  $\mu m$  thickness around a granular embryonic matrix (Fig. 7J). In the given sample a 0.45  $\mu m$  cortex layer can be distinguished from the main layer with an uneven inner surface.

Fig. 5. Surface fine structure and inner structures of branchiopod cysts: Notostraca. A, C, E, G. *Triops cancriformis*; ▷ B, D, F, H. *Lepidurus apus*; A, B. μCT selected plane; C, D. surface rendering based on μCT, cyst shell opened; E, F. cyst surface SEM; G, H. cyst shell fractured SEM. Scale bars: A–D 100 μm; E 2 μm; F–H 20 μm.



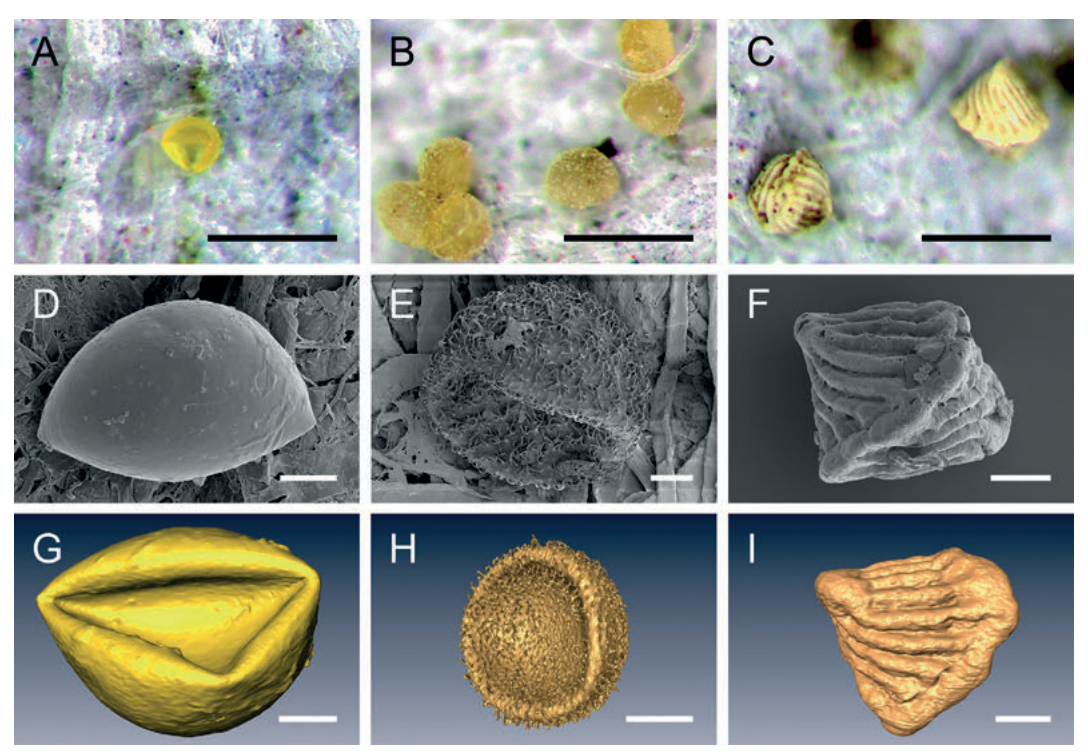


Fig. 6. Outer morphology of branchiopod cysts: Spinicaudata. A, D, G. Leptesteria dahalacensis; B, E, H. Cyzicus sp.; C, F, I. Limnadia lenticularis; A, B, C. light microscopy; D, E, F. scanning electron microscopy; G, H, I. surface rendering based on micro computed tomography. Scale bars: A–C 250 μm; D, E, G 25 μm; F, H, I 50 μm.

# Cyzicus sp.

The cysts are not completely opaque, of yellowish beige colour, and with short bent hairy protrusions on the surface (Fig. 6B, E, H). On closer SEM inspection there are tiny nipples or ridges in the order of 0.3–3  $\mu$ m (zoom into Fig. 7H). The overall shape is spherical (diameter 125–135  $\mu$ m) with a large hemispherical indentation (Figs 6H; 7B, E). As in *L. dahalacensis* the cyst shell is quite thin (ca. 1.6  $\mu$ m), enveloping a granular embryonic matrix.

#### Limnadia lenticularis

The cysts of *L. lenticularis* have size of approx. 185 x 200 μm, are opaque with a whitish yellow colour (in our samples with few brown stains and small red dots, Fig. 6C). The cyst shape is very characteristic shape (Fig. 6F, I) and can be described as made of two opposing C-shaped rounded edges in 90° orientation, interconnected by several rounded ridges (24 in our μCT rendering). The surface texture is very porous, especially on top of the ridges and edges, because the cortex layer is missing there, making the alveolar layer to appear at the surface

(Fig. 7I). The alveolar layer has a spongy structure of small interconnected chambers and with conspicuously large globular chambers underneath the ridges (Fig. 7L). Due to the special shape of the cyst the protective shell thickness varies between 5 and 27 µm, the inner layer is very thin and smooth. The embryonic cuticle is a smooth layered structure reaching hardly a thickness of 1 µm (not shown). The embryo is cup shaped (Fig. 7F) like in the other investigated species (except *B. schaefferi* and *T. stagnalis*) with a granular matrix (Fig. 7C).

#### Discussion

The task to compare large branchiopod cysts using LM, EM and CT was accomplished, the structure data are shown in Figures 1–7 in the respective image quality. Colour is accessible only by LM, surface texture depends on resolution of the imaging method, overall shape and diameter of the cysts are consistent with all 3 imaging methods. The shape of the embryo in the cyst and aspects of their internal structure and some volumetry can be shown from

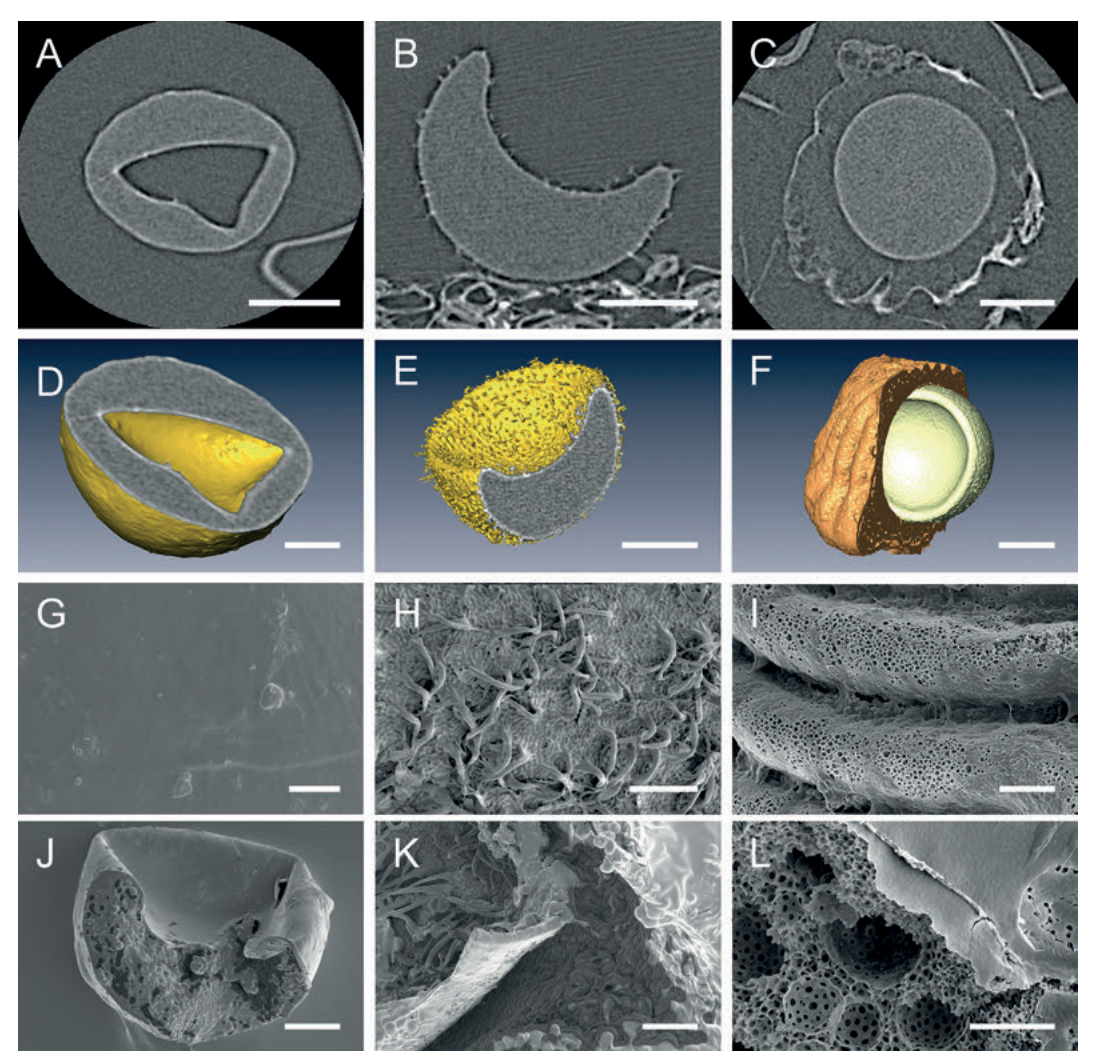


Fig. 7. Surface fine structure and inner structures of branchiopod cysts: Spinicaudata. A, D, G, J. Leptesteria dahalacensis; B, E, H, K. Cyzicus sp.; C, F, I, L. Limnadia lenticularis; A, B, C. μCT selected plane; D, E, F. surface rendering based on μCT, cyst shell opened; G, H, I. cyst surface SEM; J, K, L. cyst shell fractured SEM. Scale bars: A–C, E, F 50 μm; D, J 25 μm; G 5 μm; H, I, K 10 μm.

 $\mu$ CT data. The fine structure of the embryo surface is accessible via SEM on fractured preparations, i.e. cracked dry cysts.

# Method comparison

**Light microscopy** is effective for examining the surface colour of cysts, their size, and shape, offering a blurred impression of the surface texture. However, it does not provide high-resolution details. It shows the image of cysts like the standard observer has, without access to high-tech imaging methods.

Scanning electron microscopy (SEM) delivers high-resolution images of the external morphology of cysts, particularly highlighting the outer layers and details of ruptured samples. This method is essential for understanding fine structural features of biological specimens, including branchiopod cysts. Epibionts such as pennate diatoms from the habitat or from the culture also occasionally come to "light" (here e.g. in *Tanymastix, Chirocephalus, Lepidurus, Triops*), or any kind of sediment or dried dirt from outside (here e.g. between the bristles of *Chirocephalus*, Fig. 3C, E).

Micro-computed tomography (μCT) is a powerful, non-destructive imaging technique that enables the acquisition of 3D data for both external and internal structures of intact cysts at medium resolution and contrast. It has been used effectively to analyse porous structures in biological materials, revealing crucial microstructural properties while avoiding artifacts associated with traditional sectioning methods (Doan et al. 2012, Hamba et al. 2012). Additionally, μCT allows for volumetric assessments similar to those applied in bone structure studies (Heitzer et al. 2024).

# Comparative analysis of techniques

While SEM provides the most detailed insights into the surface morphology of cysts, µCT is ideal for creating comprehensive 3D models that represent the overall structure of the cysts. Binocular microscopy is useful for examining larger cysts, such as those of *T. cancriformis* and *L. apus*, but is less effective for smaller cysts like those of *L. dahalacensis*, *L. lenticula*ris, or Cyzicus sp., because of limited spatial resolution. The comparison shows, that some caution is required when assessing fine surface structures with low-resolution methods (cf. shape of the ridges in *E*. schaefferi in Fig. 1B, E, H). This can also apply to the inner cyst shell architecture (cf. aspect of *T. stagnalis* alveolar layer in Fig. 2L (SEM) and 2C ( $\mu$ CT) – in the latter the cortex is clearly visible, but the alveolar layer less clear).

#### **Evolutionary and ecological aspects**

Cysts are a resilient life stage for large branchiopods, enabling survival under harsh environmental conditions. The extraordinarily high resilience of the cysts of *T. cancriforms* in particular was demonstrated even under space conditions as part of the Biomex experiment on the ISS. After approximately 19 months of exposure in space, hatch rates of 10–40% were observed in the evaluation under terrestrial conditions (Zierold, oral communication). The special structure of the cysts and the physiological state of the "resting" embryo make this possible.

Insights into their evolutionary strategies emerge from combined  $\mu$ CT and SEM analyses, revealing adaptations to fluctuating environments. Gueriau et al. (2016) highlight that morphological and ecological stasis in branchiopod crustaceans has been observed over millions of years, indicating a remarkable resilience to environmental changes. Our comparative studies highlight both similarities and significant structural differences across species. For example, cysts of *Triops* sp. show greater variability in size and shape, reflecting adaptations to diverse

environmental conditions (De Walsche et al. 1991). Fryer & Boxshall (2009) describe the specialized feeding mechanisms of *Lynceus*, which highlight the ecological adaptations of branchiopods to their environments.

Research has revealed significant intraspecific variation in cysts size among large branchiopods, often influenced by geographical and environmental factors (Zierold et al. 2007, 2009). For instance, larger eggs are typically produced in colder climates, enhancing the survival of newly hatched larvae (Czyż et al. 2016). This variation highlights how local conditions shape the reproductive strategies of these species (Velonà et al. 2009). Additionally, salinity levels critically affect hatching success, with elevated salinity potentially reducing the viability of dormant eggs (Mabidi et al. 2018).

The morphology of large branchiopod cysts assists in species identification. Studies indicate substantial inter- and intrapopulation morphological variations across species, serving as valuable taxonomic indicators (Padhye et al. 2016). Furthermore, large branchiopods play pivotal ecological roles in temporary wetlands, influencing community dynamics through interactions such as predation and competition (Waterkeyn et al. 2011).

The dispersal mechanisms of large branchiopods are also significant. Their cysts can be transported by various vectors, including waterfowl and terrestrial mammals, facilitating distribution across ephemeral habitats (Vanschoenwinkel et al. 2008, Schwentner et al. 2012). This ability to disperse is crucial for maintaining genetic diversity and colonizing new environments, especially in fragmented landscapes (Waterkeyn et al. 2009). Their presence in diverse habitats, such as temporary ponds in Apulia, Italy, highlights their ecological flexibility (Alfonso 2017). Some species are even found in artificial water bodies like carp ponds, which may serve as secondary habitats replacing former floodplain areas (Barthelmes 1963, Vogelmann et al. 2021a).

# Shape and structure differences

Freshly laid cysts typically exhibit a distinctly spherical shape (with the exception of *Tanymastix*: here the cysts already have their typical lens-shaped shape in the egg sac of the female before they are deposited). However, during the drying process, this shape changes in some species, particularly in *Artemia monica*, *Cyzicus* sp., and *L. dahalacensis*, where the cysts collapse, resulting in larger indentations (Figs 3B,D; 6D,G,E,H). In contrast, this phenomenon is less pronounced in *B. schaefferi* where surface folds become more prominent in the dry state, or absent in other species.

The elongate processes in the subcortical spaces of *B. schaefferi* are found to connect cortex and alveolar layer in the edges, and appear to be torn during the opening process of the spaces, either as a regular developmental process or as a consequence of shrinkage.

The stability of the cysts is influenced by the structure and composition of the cyst shell. Thin shells with poorly structured middle layers\* lead to instability and collapse as water content decreases. Conversely, when dried cysts are reintroduced to water, they swell and regain their original spherical shape, indicating a reversible process (\* in *Leptesteria* and *Cyzicus* a differentiation into these layers was not possible and further clarification should be carried out in connection with the hatching process).

Inspecies such as T. cancriformis, L. apus, and L. lenticularis,  $\mu$ CT examinations reveal that their external shape remains unchanged in the dry state. However, the embryonic cell mass within the cyst adopts a cupshaped formation (Figs 2E, 5C–D, 7F). Additionally we find a narrow "empty" space in the anostracan species investigated with  $\mu$ CT (Fig. 2A–C) between inner shell layer and embryonic cuticle. In the Notostraca and Limnadia these structures touch each other.

This suggests that a well-developed cyst shell and partly rib-like reinforcements prevent collapse during water loss. Despite these structural advantages, the viability of individual species under natural conditions remains unaffected, as the hatching ability from laid cysts appears stable.

#### Comparison to other studies

When comparing *L. lenticularis* and *T. cancriformis*, the former displays smaller, more streamlined cysts that may enhance dispersal in temporary water bodies (Czyż et al. 2016). These morphological differences likely relate to their life histories, with *Triops* investing more in cyst size to increase larval survival in unpredictable environments (Zierold et al. 2007).

Notostracan cysts are significantly larger than those of anostracans or diplostracans. Thiéry & Gasc (1991) noted that notostracan cysts exceed 400 µm in diameter, while anostracan cysts range from 230–380 µm, and diplostracan cysts are typically smaller than 200 µm. Our observations confirm that *L. apus* cysts are larger than those of *T. cancriformis*, aligning with Vogelmann et al. (2021b), who noted that *T. cancriformis* cysts exceed 500 µm. Additionally, our images reveal a thicker tertiary alveolar layer in *T. cancriformis* than previously described by Engelmann & Hahn (2004).

In contrast, *L. apus* exhibits a unique strategy: its cysts are covered with an adhesive-like substance on the shell surface. As a result, newly laid cysts adhere

to sediment particles or plant material in the substrate. This adhesive substance forms the outer layer of the cyst and hardens shortly after being deposited in water. Once hardened, the particles attached to the cyst surface are so firmly bonded that attempts to remove them often damage the outer shell (see Figs 4D, 5B, where areas of diffusely hardened adhesive material are visible; attached particles could be partially removed).

It is plausible that cysts adhering to substrate particles are less likely to be swept away by water currents in temporary flood pools. In addition to this protective function, the "rough" surfaces seen on cysts of species such as *Chirocephalus carnuntanus* and *Cyzicus* sp. (Figs 3C, 6E) may aid in anchoring the cysts to the substrate. Such textures could also play a role in facilitating transport by vectors like birds.

The  $\mu$ CT images of *L. apus* suggest sediment adhesion to the outer cyst shell, contributing to a more heterogeneous surface appearance. The alveolar structure in both *T. cancriformis* and *L. apus* is clearly visible in SEM images of burst cysts. Mitchell (1990, in Kuller & Gasith) proposes that this structure facilitates flotation upon drying, which may enhance hatching at higher temperatures.

Furthermore, studies by Thiéry & Gasc (1991) describe *Cyzicus tetracerus* cysts in a manner similar to our findings, particularly regarding their "hairy structure". However, this feature is less discernible in their images. Studies by Czyż et al. (2016) also include images of *Cyzicus*, although with less detail than ours. Our SEM and µCT images clearly illustrate the cysts' surface patterns, corroborating previous findings on structural variations within populations, likely due to geographic or climatic factors (Belk 1977, Mura 1992, Brendonck & Coomans 1994a, b).

Gilchrist (1978) supports our observations of B. schaefferi, reporting cyst diameters of 0.25 mm. The wrinkled structure visible in our SEM images aligns with these findings and is also evident in our  $\mu$ CT images, although SEM better highlights the surface pores. Our images of T. stagnalis provide comprehensive representations of this species across all three methods, illustrating variations in size and diameter based on origin, consistent with studies by Mura (1986).

Finally, the cysts of *L. lenticularis* are typically reported as 290–370  $\mu$ m in diameter, while our images indicate slightly smaller sizes. In contrast, the cysts of *L. dahalcencis* are relatively featureless. Padhye et al. (2016) and Thiéry & Gasc (1991) distinguish Leptestheriidae species based on their spherical appearance, contrasting with the elongated, structureless cysts of *L. dahalcencis*. Our  $\mu$ CT images provided clear morphological insights, despite the absence of detailed surface features.

#### Conclusion

In conclusion, each imaging technique –  $\mu$ CT, SEM, and binocular microscopy – has its strengths and weaknesses, offering unique insights into cyst morphology. Our findings align with previous studies, while providing more detailed insights into the structural differences across species. These imaging techniques are complementary, and together they enhance our understanding of cyst adaptations and their ecological significance.

All examined native species have distinctly different cysts that allow for species identification. This makes it possible to assign isolated cysts from soil samples in dried-out habitats to their respective species. Since it can take years for such habitats to refill with water, enabling a new generation of large branchiopods to emerge, the ability to conduct such studies during these dry intervals is highly relevant for faunistic and ecological surveys, last but not least in times of rising global temperatures.

# Acknowledgements

We would like to express our gratitude to Stephan Scholz and Christian Wirkner (Allgemeine und Spezielle Zoologie, Universität Rostock) for carrying out the Xradia scans. Special thanks to Sebastian Buchert, René & Ellen Driechciarz, Christian Eichinger, and Jan Venzlaff for providing alive specimens for cyst collection efforts. The ZEISS Xradia 410 Versa at Universität Rostock was jointly sponsored by the Deutsche Forschungsgemeinschaft (DFG, German research foundation – INST264/130-1 FUGG) and Land Mecklenburg-Vorpommern; the ApreoVS at LMU Munich was supported by Deutsche Forschungsgemeinschaft (DFG) – INST86/1940-1 FUGG and Land Bayern.

#### References

- Alfonso, G. 2017. Diversity and distribution of large branchiopods (Branchiopoda: Anostraca, Notostraca, Spinicaudata) in Apulian ponds (SE Italy). The European Zoological Journal 84: 172–185. https://doi.org/10.1080/24750263.2017.1294628
- Barthelmes, D. 1963. Massenentwicklung des Kiemenfußkrebses *Triops cancriformis* in Karpfenteichen und die Möglichkeit einer Bekämpfung. Deutsche Fischerei Zeitung 10: 330–332.
- Belk, D. 1977. Evolution of egg size strategies in fairy shrimp. The Southwestern Naturalist 22: 99–105.
- Brendonck, L. & Coomans, A. 1994a. Egg morphology in African Streptocephalidae (Crustacea, Branchiopoda, Anostraca). Part I. South of Zambezi and Kunene rivers, and Madagascar. Archiv für Hydrobiologie 99: 313–334.

- Brendonck, L. & Coomans, A. 1994b. Egg morphology in African Streptocephalidae (Crustacea, Branchiopoda, Anostraca). Part II. North of Zambezi and Kunene rivers. Archiv für Hydrobiologie 99: 335– 356.
- Burmeister, E.-G. 2000. Die Besiedlungsstrategie cystobionter Krebse und ihre Fundorte in Bayern Crustacea: Notostraca, Anostraca, Conchostraca. Bericht der Naturforschenden Gesellschaft Augsburg 59: 1–38.
- Clegg, J. S. 1997. Embryos of *Artemia franciscana* survive four years of continuous anoxia: the case for complete metabolic rate depression. Journal of Experimental Biology 200(3): 467–475.
- Czyż, M. J., Woliński, P. & Goldyn, B. 2016. Cyst morphology of large branchiopod crustaceans (Anostraca, Notostraca, Laevicaudata, Spinicaudata) in western Poland. Biological Letters 53 (2): 79–88.
- De Walsche, C., Munuswamy, N. & Dumont, H. J. 1991. Structural differences between the cyst walls of Streptocephalus dichotomus (Baird), S. torvicornis (Waga), and Thamnocephalus platyurus (Packard) (Crustacea: Anostraca), and a comparison with other genera and species. Hydrobiologia 212: 195– 202. https://doi.org/10.1007/bf00026001
- Doan, H. D., Delage, P., Nauroy, J. F., Tang, A. M. & Youssef, S. 2012. Microstructural characterization of a Canadian oil sand. Canadian Geotechnical Journal 49 (10): 1212–1220. https://doi.org/10.1139/ t2012-072
- Driechciarz, R., Driechciarz, E., Pellmann, H., Venzlaff, J., Grabow, K., Martens, A. & Engelmann, M. 2025. First record of *Chirocephalus carnuntanus* (Brauer, 1877) (Branchiopoda, Anostraca) from Germany. Crustaceana 98 (7–8): 725–735. https://doi.org/10.1163/15685403-bja10474
- Engelmann, M. & Hahn, T. 2004. Vorkommen von Lepidurus apus, Triops cancriformis, Eubranchipus (Siphonophanes) grubii, Tanymastix stagnalis und Branchipus schaefferi in Deutschland und Österreich (Crustacea: Notostraca und Anostraca). Faunistische Abhandlungen des Museums für Tierkunde in Dresden 25: 3–67.
- Fryer, G. & Boxshall, G. 2009. The feeding mechanisms of *Lynceus* (Crustacea: Branchiopoda: Laevicaudata), with special reference to *L. simiaefacies* Harding. Zoological Journal of the Linnean Society 155: 513–541. https://doi.org/10.1111/j.1096-3642.2008.00455.x
- Gilchrist, B. M. 1978. Scanning electron microscope studies of the egg shell in some Anostraca (Crustacea: Branchiopoda). Cell and Tissue Research 193: 337–351.
- Glandt, D. 2006. Praktische Kleingewässerkunde. Zeitschrift für Feldherpetologie, Supplement 9, 200 pp., Bielefeld (Laurenti-Verlag).
- Gottwald, R. & Hödl, W. 1996. Zur Phänologie von Groß-Branchiopoden der unteren March-Auen. Stapfia 42: 51–57.

- Gueriau, P., Rabet, N., Clément, G., Lagebro, L., Vannier, J., Briggs, D. E. G., Charbonnier, S., Olive, S. & Béthoux, O. 2016. A 365-million-year-old freshwater community reveals morphological and ecological stasis in branchiopod crustaceans. Current Biology 26 (3): 383–390. https://doi.org/10.1016/j.cub.2015.12.039
- Hamba, H., Nikaido, T., Sadr, A., Nakashima, S. & Tagami, J. 2012. Enamel lesion parameter correlations between polychromatic micro-CT and TMR. Journal of Dental Research 91 (6): 586–591. https://doi.org/10.1177/0022034512444127
- Heitzer, M., Winnand, P., Ooms, M., Magnuska, Z., Kiessling, F., Buhl, E. M., Hölzle, F. & Modabber, A. 2024. A biodegradable tissue adhesive for post-extraction alveolar bone regeneration under ongoing anticoagulation – a microstructural volumetric analysis in a rodent model. International Journal of Molecular Sciences 25(8): 4210. https:// doi.org/10.3390/ijms25084210
- Mabidi, A., Bird, M. S. & Perissinotto, R. 2017. Distribution and diversity of aquatic macroinvertebrate assemblages in a semi-arid region earmarked for shale gas exploration (Eastern Cape Karoo, South Africa). PLOS One 12 (6): e0178559. https://doi.org/10.1371/journal.pone.0178559
- Mabidi, A, Bird, M. S. & Perissinotto, R. 2018. Increasing salinity drastically reduces hatching success of crustaceans from depression wetlands of the semi-arid Eastern Cape Karoo region, South Africa. Scientific Reports 8 (1): 5983. https://doi.org/10.1038/s41598-018-24137-0
- Mitchell, S. A. 1990. Factors affecting the hatching of Streptocephalus macrourus Daday (Crustacea, Eubranchiopoda) eggs. Hydrobiologia 194: 13–22.
- Mura, G. 1986. SEM morphological survey on the egg shell in the Italian anostracans (Crustacea, Branchiopoda). Hydrobiologia 134: 273–286.
- Mura, G. 1992. Additional remarks on cyst morphometrics in anostracans and its significance. Part II: Egg morphology. Crustaceana 63: 225–246.
- Olesen, J. 2007. Monophyly and phylogeny of Branchiopoda, with focus on morphology and homologies of branchiopod phyllopodous limbs. Journal of Crustacean Biology 27 (2): 165–183.
- Olesen, J. & Richter, S. 2013. Onychocaudata (Branchiopoda: Diplostraca), a new high-level taxon in branchiopod systematics. Journal of Crustacean Biology 33(1): 62–65.
- Padhye, S., Timms, B. & Ghate, H. V. 2016. Large branchiopod (Crustacea: Branchiopoda) egg morphology of Western Ghats, Maharashtra, India. Zootaxa 4079 (2): 246–254. https://doi.org/10.11646/zootaxa.4079.2.6
- Rieder, N., Grössle, L., Havelka, P. & Ott, H. 1979. Über das Auftreten einiger seltener Blattfußkrebse im Raum Karlsruhe (*Triops cancriformis* Bosc, *Limnadia lenticularis* (Linnaeus), *Siphonophanes grubei* (Dybowski)). Beiträge zur Naturkundlichen Forschung in Südwest-Deutschland 38: 135–139.

- Schwentner, M., Timms, B. V. & Richter, S. 2012. Flying with the birds? Recent large-area dispersal of four Australian *Limnadopsis* species (Crustacea: Branchiopoda: Spinicaudata). Ecology and Evolution 2: 1605–1626. https://doi.org/10.1002/ece3.265
- Simon, L. 2016. Rote Liste und Gesamtartenliste der Blattfußkrebse (Branchiopoda: Anostraca, Conchostraca, Notostraca) Deutschlands. Naturschutz und Biologische Vielfalt 70: 367–378.
- Thiéry, A. & Gasc, C. 1991. Resting eggs of Anostraca, Notostraca and Spinicaudata (Crustacea, Branchiopoda) occurring in France: identification and taxonomical value. Hydrobiologia 212: 245–259. http://dx.doi.org/10.1007/BF00026008
- Thiéry, A., Brtek, J. & Gasc, C. 1995. Cyst morphology of European branchiopods (Crustacea, Anostraca, Notostraca, Spinicaudata, Laevicaudata). Bulletin du Muséum National d'Histoire Naturelle, 4º Série, 17 (1–2): 107–139. https://doi.org/10.5962/p.290318
- Vanschoenwinkel, B., Waterkeyn, A., Vandecaetsbeek, T., Pineau, O., Grillas, P. & Brendonck, L. 2008. Dispersal of freshwater invertebrates by large terrestrial mammals: a case study with wild boar (*Sus scrofa*) in Mediterranean wetlands. Freshwater Biology 53: 2264–2273. https://doi.org/10.1111/j.1365-2427.2008.02071.x
- Velonà, A., Luchetti, A., Scanabissi, F. & Mantovani, B. 2009. Genetic variability and reproductive modalities in European populations of *Triops cancri*formis (Crustacea, Branchiopoda, Notostraca). Italian Journal of Zoology 76: 366–375. https://doi. org/10.1080/11250000902785314
- Vogelmann, C., Dunst, J., Krause, S., Tsalkatis, A., Grabow, K. & Martens, A. 2021b. Nachweis von Groß-Branchiopoden (Crustacea: Anostraca, Notostraca und Diplostraca) am Oberrhein anhand von Bodenproben und ihr Vergleich mit tatsächlichen Funden bei Hochwasser. Abhandlungen und Berichte für Naturkunde, Museum für Naturkunde Magdeburg 36: 161–168.
- Vogelmann, C., Másílko, J. & Oberle, M. 2021a. Leptestheria dahalacencis in einer Karpfenzucht in Bayern (Crustacea: Diplostraca). Abhandlungen und Berichte für Naturkunde, Museum für Naturkunde Magdeburg 36: 73–77.
- Wang, C.-C. & Chou, L.-S. 2015. Terminating dormancy: hatching phenology of sympatric large branchiopods in Siangtian pond, a temporary wetland in Taiwan. Journal of Crustacean Biology 35(3): 301–308. https://doi.org/10.1163/1937240x-00002322
- Waterkeyn, A., Grillas, P., de Roeck, E. R. M., Boven, L. & Brendonck, L. 2009. Assemblage structure and dynamics of large branchiopods in Mediterranean temporary wetlands: patterns and processes. Freshwater Biology 54: 1256–1270. https:// doi.org/10.1111/j.1365-2427.2009.02174.x
- Waterkeyn, A., Vanschoenwinkel, B., Vercampt, H., Grillas, P. & Brendonck, L. 2011. Long-term effects of salinity and disturbance regime on active

- and dormant crustacean communities. Limnology and Oceanography 56: 1008–1022. https://doi.org/10.4319/lo.2011.56.3.1008
- Wiggins, G. B., Mackay, R. J. & Smith, I. M. 1980. Evolutionary and ecological strategies of animals in annual temporary pools. Archiv für Hydrobiologie, Supplement 58: 97–206.
- Wüstemann, O. & Nicolai, B. 2012. Zum Vorkommen und zur Ökologie der Kiemenfußkrebse (Crustacea, Branchiopoda) *Branchipus schaefferi* Fischer 1934, und *Triops cancriformis* (Bosc, 1801) auf dem ehemaligen Truppenübungsplatz südlich Halberstadt (Sachsen-Anhalt). Abhandlungen und Berichte aus dem Museum Heineanum 9: 127–139.
- Zierold, T., Hänfling, B. & Gómez, Á. 2007. Recent evolution of alternative reproductive modes in the 'living fossil' *Triops cancriformis*. BMC Evolutionary Biology 7: 161. https://doi.org/10.1186/1471-2148-7-161
- Zierold, T., Montero-Pau, J., Hänfling, B. & Gómez, Á. 2009. Sex ratio, reproductive mode and genetic diversity in *Triops cancriformis*. Freshwater Biology 54 (7): 1392–1405. https://doi.org/10.1111/j.1365-2427.2009.02191.x